bioRxiv preprint doi: https://doi.org/10.1101/803973; this version posted October 14, 2019. The copyright holder for this preprint (which was not certified by peer review) is the author/funder. All rights reserved. No reuse allowed without permission.

STEM CELL ACTIVITY AND REGENERATION IN ROOTS REQUIRE NON-CELL AUTONOMOUS REGULATION FROM THE GROUND TISSUE

Alvaro Sanchez-Corrionero[1*], Pablo Perez-Garcia[1*], Javier Cabrera[1*], Javier Silva-Navas[1#], Juan Perianez-Rodriguez[1##], Inmaculada Gude[1], Juan Carlos del Pozo[1], Miguel A. Moreno-Risueno[1§].

[1]Centro de Biotecnología y Genómica de Plantas (Universidad Politécnica de Madrid – Instituto Nacional de Investigación y Tecnología Agraria y Alimentaria), Madrid, Spain

[*] These authors equally contributed to this work

[#] Current address: Department of Plant Molecular Biology, University of Lausanne, 1015 Lausanne, Switzerland. [##] Current address: Departamento de Biología y Geología, Física y Química Inorgánica, Universidad Rey Juan Carlos, E-28933 Móstoles, Spain.

[§] Corresponding author: miguelangel.moreno@upm.es.

Keywords: plant stem cells; plant regeneration; organ patterning; mobile transcription factor; cell fate specification

ABSTRACT

Stem cells are central to plant development. Root stem cells organize around the quiescent center (QC) and give rise to cell lineages that generate the root radial pattern during postembryonic development. Here, through analyses of *Arabidopsis thaliana* mutants in the transcription factors BLUEJAY, JACKDAW and SCARECROW and chemical treatments, we have found that QC regenerative capacities maintain the stem cell niche during postembryonic development; and in addition, specification of QC cells are required to re-establish the radial pattern upon wounding. Our data shows that QC functionality in maintaining and regenerating the radial pattern requires non-cell-autonomous regulation by transcription factors BLUEJAY, JACKDAW and SCARECROW. We observe that these factors regulate auxin transport, auxin maxima formation, as well as the stem cell regulator SHORT-ROOT from the ground tissue. We tracked this non-cell-autonomous regulation to C-REPEAT BINDING FACTOR 3 (CBF3). CBF3 protein is mobile, while *CBF3* gene is expressed in the ground tissue downstream of BLUEJAY, JACKDAW and SCARECROW. Targeted-expression of *CBF3* to the ground tissue of *blj jkd scr* mutant recovers radial patterning and, upon laser ablation, stem cell niche regeneration and tissue organization in layers. CBF3 also regulates QC organization and inhibits stem cell niche differentiation. We propose CBF3 may function as a radial signal maintaining stem cell niche activity and regeneration.

bioRxiv preprint doi: https://doi.org/10.1101/803973; this version posted October 14, 2019. The copyright holder for this preprint (which was not certified by peer review) is the author/funder. All rights reserved. No reuse allowed without permission.

INTRODUCTION

Plant developmental plasticity relies on meristems. Meristems are formed by highly reprogrammable proliferative cells organized in layers or cell types, which generate from the activity of stem cells during postembryonic development (1). Stem cells are found in specific microenvironments within meristems called stem cell niches (2, 3). Stem cell niches also contain organizer cells which promote stem cell activity and maintain surrounding cells in an undifferentiating state (4). Organizer cells of the root stem cell niche are called the quiescent center (QC) because of their slow division rate (5). Root stem cells have pre-assigned identities and thus they are understood as initial cells of the distinctive cell type lineages of the root. Root initials divide asymmetrically to generate daughter cells, which show high proliferation capacity (6). The combined activity of the root stem cells/initials and their daughters maintains meristem size and function replacing cells entering into differentiation. The radial organization of cell lineages in layers is not fully understood.

Root stem cell niche specification and positioning in *Arabidopsis thaliana* requires hormone gradients and other signals, primarily converging into the PLETHORA (PLT) and SHORT-ROOT (SHR)/SCARECROW (SCR) pathways (2, 7-9). Auxin hormone forms a gradient in the root meristem with a maximum in the stem cell niche (10). PLT accumulation is interpreted as a slow-read of auxin maxima, and thus, a maximum in the accumulation of PLT proteins occurs in the stem niche area. PLT transcription factors (TFs) are mobile proteins, moving longitudinally in oppose direction to the auxin gradient. PLT function is dose dependent and high PLT concentration associates with stem cell niche specification and QC maintenance, whereas decreasing PLT concentrations may instruct cells to proliferate and finally differentiate (8, 11, 12). SHR is also a mobile TF. *SHR* is expressed in the central vasculature cylinder and surrounding pericycle layer (13), although the mechanism controlling its transcription is not resolved. SHR protein moves radially to adjacent endodermis and QC, where it activates its targets SCR and the TF of the BIRD family JACKDAW (JKD) (14, 15), functioning as a dose dependent signal (16). SCR and JKD interact with SHR and sequester it in nuclei, which is necessary to establish important aspects of root cell type organization in the radial axis or radial patterning, such as endodermis/cortex and metaxylem/protoxylem formation from division of preexistent cell lineages (17-19). SHR, SCR and JKD have been reported to cell-autonomously maintain and promote QC specific expression and activity (2, 20). SCR also regulates gibberellin and cytokinin signaling required for root stem cell activity in the QC and, in addition cytokinin signaling from the endodermis (21-23). SCR mediated regulation of

bioRxiv preprint doi: https://doi.org/10.1101/803973; this version posted October 14, 2019. The copyright holder for this preprint (which was not certified by peer review) is the author/funder. All rights reserved. No reuse allowed without permission.

cytokinin signaling, which eventually affects auxin biosynthesis, regulates meristem size and root growth

WUSCHEL-RELATED HOMEODMAIN 5 (WOX5) is involved in specification of QC identity and to maintain a low degree of differentiation of surrounding stem cells (4). PLT, SHR, JKD and SCR TFs regulate *WOX5* expression (5, 8, 9, 20). In addition, PLT and SCR interact with the TFs TEOSINTE-BRANCHED CYCLOIDEA PCNA (TCP) 20 and 21 to regulate *WOX5* expression through PLT binding sites in *WOX5* promoter (24). REPRESSOR OF WUSCHEL1 (ROW1) and a circuit form by CLAVATA3-ESR RELATED 40 (CLE40), CLAVATA1 (CLV1) and ARABIDOPSIS CRINKLY 4 (ACR4) restrict *WOX5* expression to the QC within the stem cell niche (25, 26). Interestingly, WOX5 protein can move to adjacent distal stem cells to regulate their differentiation state (27)

Wounded or ablated cells can be replaced by adjacent meristematic cells, which are highly reprogrammable (28, 29) During standard growth, QC cells may also divide to replenish dead stem cells, however, this is restricted by RETINOBLASTOMA-RELATED (RBR) protein / SCR circuit and WOX5 working as repressors of mitotic transitions and CYCLIN D activity, respectively (5, 30). Regenerative QC divisions can be induced upon supplementation with genotoxic agents that selectively kill stem cells, showing that the QC may function as a reservoir for stem cells (31, 32). WOX5, SCR and PLT play a major role during regenerative processes. Removal of QC cells through laser wounding triggers the specification of a new stem cell niche involving WOX5, SCR and PLT as regulators of cell fate and auxin gradient formation (33).

In this paper we describe a non-cell-autonomous role for SCR, JKD and another BIRD TF BLUEJAY (BLJ) in maintaining the stem cell niche through their downstream-regulated TF C-REPEAT BINDING FACTOR 3 (CBF3). CBF3, which was originally described as a cold response factor, shows specific expression in the ground tissue under standard temperature, while CBF3 protein is mobile. In the absence of BLJ, JKD and SCR, we detect loss of QC cells and decreased QC regenerative capacities, which lead to progressive loss of cell layers and tissues. In addition, BLJ, JKD and SCR regulate SHR protein levels, Targeted expression of *CBF3* to the ground tissue of *blj jkd scr* mutant shows recovery of the stem cell niche and stem cell regeneration. As SHR is transcribed in vasculature regions and we found that CBF3 regulates SHR protein levels, our results indicate that CBF3 may work as a radial signal from the ground tissue to regulate stem cell niche specification and regeneration.

bioRxiv preprint doi: https://doi.org/10.1101/803973; this version posted October 14, 2019. The copyright holder for this preprint (which was not certified by peer review) is the author/funder. All rights reserved. No reuse allowed without permission.

RESULTS

BLUEJAY, JACKDAW and SCARECROW work combinedly to maintain the Arabidopsis root meristem and the radial pattern.

We investigated root growth in loss of function mutants for the C_2H_2 TFs collectively known as the BIRDs. We observed reduced growth in plants carrying *bluejay (blj)* and *jackdaw-4 (jkd)* mutations (Fig. 1A). *scarecrow (scr)* mutant has been described to regulate meristem function and root growth (7). Combination of *blj*, *jkd4* and *scr4* mutations showed additive defects, which resulted in almost root growth cessation from 8 days post imbibition (dpi) onwards (Fig. S1A-B). *short-root (shr)* and *plethora (plt)* mutants, which are defective in stem cell niche maintenance and meristem function, also show reduced root growth (9, 13). Our data show that *blj jkd scr* mutants continuously decreased growth, while *plt1 plt2* tended to maintain certain growth over all days analyzed. Triple mutants *shr plt1 plt2* stopped growth at 7 dpi. Meristem inspection showed that although meristems of *blj jkd scr* mutants were of similar size as wild type (WT) prior germination (Fig. S1C), by 6 dpi meristems of *blj jkd scr* were less than half the size of those of WT and almost of similar size as *plt1 plt2* meristems (Fig. S1D-E). From 7 to 13 dpi *blj jkd scr* meristems further reduced their size, becoming even smaller than those of *shr* and *plt1 plt2* while all *shr plt1 plt2* meristems had differentiated. Because defects appeared from 6 dpi onwards, we report results in rest of the paper between 6 and 13 dpi, normally at the first day it was detected or when it was most obvious.

Triple mutant *blj jkd scr* has been reported to show radial patterning defects (15). Analysis of *blj jkd scr* meristems between 8 and 13 dpi showed profound alteration of the radial patterning. Transverse sections of *blj jkd scr* at 8 dpi showed no easily recognizable organization in concentric layers with central cells showing palisade arrangement. *scr* and *jkd scr* showed radial pattern organization in concentric layers, although with reduced number of layers as compared to the WT (Fig. 1B-C). BLJ, JKD and SCR proteins accumulate in the ground tissue; and in addition, JKD and SCR protein are present in the QC (15). As *blj jkd scr* mutants show severe disruption of the normal radial pattern while organization in concentric layers was still present in *jkd scr* mutants, a non-cell autonomous mechanism regulating layer organization from the ground tissue can be inferred. Furthermore, at 13 dpi only a few enlarged cells made up the *blj jkd scr* root cylinder, suggesting reduced capacity of *blj jkd scr* meristems to renovate and pattern themselves during postembryonic development (Fig. 1D).

bioRxiv preprint doi: https://doi.org/10.1101/803973; this version posted October 14, 2019. The copyright holder for this preprint (which was not certified by peer review) is the author/funder. All rights reserved. No reuse allowed without permission.

To better understand defects in *blj jkd scr* we performed data mining using microarray experiments which profiled the *blj jkd scr* apical meristem at 5dpi (15), prior severe growth decrease was observed. Analysis of differentially expressed genes between wild type (WT) and *blj jkd scr* meristems showed repression of genes involved in regulation of cell cycle progression (Fig. S2A), among others. Introgression of the G2 to M marker CYCB1;1 in *blj jkd scr* showed severe impairment in mitotic transition (Fig. S2B), likely indicative of less cell proliferation rate. Cell proliferation rate impacts meristem size. Further analyses of differentially expressed genes in the *blj jkd scr* apical meristem showed repression of meristematic genes. In addition, we observed activation of genes normally expressed in the differentiation zone (Fig. 1E, Fig. S2C-D). When we investigated differentiation, we observed meristem exhaustion for *blj jkd scr* mutants between 8-13 dpi as compared to the WT, while it occurred later for *jkd scr, shr* and *plt1 plt2* mutants (Fig. 1F).

Tissue organization in layers involves BLUEJAY, JACKDAW, SCARECROW and quiescent center cells

To further investigate patterning defects observed in *blj jkd scr*, we introgressed tissue and stem cell markers into this mutant. Our results show localization of the stem cell differentiation marker SOMBRERO (SMB) – GFP in cells located in the position of distal stem and QC cells, while SMB-GFP is typically excluded from QC cells as observed in the WT (Fig. 2A). In addition, we observed that WUSCHEL RELATED HOMEOBOX (WOX) 5-GFP, which primarily marks QC cells, was expressed in reduced number of cells in *blj jkd scr* at 6 dpi as compared to the WT (Fig. 2B). These results indicate a more differentiated state of the stem cell niche in *blj jkd scr* with reduced number of QC cells.

Reduced number of QC cells could result in less stem cell activity but also in less regenerative capacity of the QC to replace non-functional or damaged stem cells. To test this hypothesis, we treated WT roots with genotoxic drug bleomycin. Bleomycin was shown to cause stem cell death (31, 32). However, we observed that at higher concentration than reported, QC cells could be also damaged or killed besides stem cells. After two days of treatment with this concentration, most QC cells had died in WT roots as indicated by propidium iodine staining inside the cell and absence of WOX5-GFP marker. In addition, the whole meristem appeared more differentiated showing enlarged cells and reduced number of vasculature layers (Fig. 2C). Upon removal from treatment, remaining WT QC cells divided but failed to reconstitute a normal meristem showing reduced number of tissue layers. At this stage, WT roots resembled *blj jkd scr* roots at 12 dpi (Fig. 2C-D), indicating that reduced number of QC cells may result in

bioRxiv preprint doi: https://doi.org/10.1101/803973; this version posted October 14, 2019. The copyright holder for this preprint (which was not certified by peer review) is the author/funder. All rights reserved. No reuse allowed without permission.

altered radial pattern and be the cause of the observed defects in the stem cell niche and meristem of *blj jkd scr* mutant.

BLUEJAY, JACKDAW and SCARECROW are required to maintain SHORT-ROOT protein levels.

Stem cell and QC specification requires the SHR/SCR pathway (24). As our transcriptomic analyses showed that *SHR* genes were repressed in the *blj jkd scr* apical meristem (Fig. S3A), we decided to investigate SHR protein accumulation. For this purpose, we performed signal quantification using hybrid detector counting in confocal analyses as previously shown to accurately detect changes in gene expression and protein levels (34). We did not observe differences in SHR protein levels at 3dpi, although SHR was mostly devoid from endodermis nuclei as previously observed in *scr* mutants (17). However, at 6 dpi we observed less SHR accumulation in *blj jkd scr* in comparison with the WT (Fig. 3A). Our results show that impairment in number of QC cells, meristematic function and patterning in *blj jkd scr* aggravates from 6dpi onwards, which interestingly correlates with SHR protein decrease.

QC specification has been described as a slow readout of auxin maxima accumulation (11). In order to investigate whether impairment in auxin gradient and maxima formatin in *blj jkd scr* could explain the observed defects in the QC, we analyzed auxin efflux carrier expression. Our transcriptomic analyses showed decrease in *PIN1*, *PIN2* and *PIN4* gene expression (Fig. S3B). PIN1 and PIN4 are essential for formation of a functional auxin gradient at the root tip (35). Analysis of PIN1 and PIN4 protein accumulation in *blj jkd scr* showed decrease in the amount of PIN1 and PIN4 proteins (Fig. 3B, C). In addition, we also detected less auxin response in *blj jkd scr* as reported by the *DR5* marker (Fig. 3D). BLJ is specifically localized in the ground tissue, while JKD and SCR accumulate both in the ground tissue and QC cells (15). As *PIN1* and *PIN4* genes are expressed in the vasculature and columella, our results indicate a non-cell-autonomous effect on auxin transporters by BLJ, JKD and SCR. As a result, this could lead to impairment in maintaining the auxin gradient. SHR protein is generated in the vasculature. As BLJ, JKD and SCR are not located in this region either, they must also regulate *SHR* expression through a non-cell-autonomous mechanism.

Identification of ground tissue transcription factors as mobile putative signals

To identify putative signals involved in non-cell-autonomous regulation from the ground tissue, we focused on the SHR pathway as BLJ, JKD and SCR are direct targets of SHR and they regulate most of the SHR responses (15). Moreover, as mobile TFs normally function as developmental cues, we selected TFs with enriched or specific

bioRxiv preprint doi: https://doi.org/10.1101/803973; this version posted October 14, 2019. The copyright holder for this preprint (which was not certified by peer review) is the author/funder. All rights reserved. No reuse allowed without permission.

expression in the ground tissue out of the SHR network (Fig. 4A). To detect if any of these TFs might be mobile we used the J0571*/GAL4-UAS::TF* system to direct expression of the identified TFs tagged with a *YFP* to the ground tissue. Out of the TF tested (Supplementary Table 1), 3 TFs C-REPEAT BINDING FACTOR 3 (CBF3), DUO1-ACTIVATED ZINC FINGER 3 (DAZ3) and NUCLEAR FACTOR Y SUBUNIT B5 (NF-YB5) showed YFP signal outside of the GT transcriptional domain (GFP marked), being this signal more noticeable in the vasculature and stem cell niche area (Fig. 4B, Fig. S4A, B). Interestingly, an abnormal radial pattern, with extra divisions in the ground tissue, was observed for these 3 J0571*/GAL4-UAS::TF* lines.

CBF3 maintains meristematic function, the stem cell niche and the radial pattern

To further explore *CBF3* expression pattern we fused three fluorescent mCherry proteins to a nuclear localization signal (NLS) and express this construct under the control of *CBF3* promoter. We found specific expression in endodermis nuclei (Fig. 4C). Interestingly, although *CBF3* expression associates with cold response (36), we found that *CBF3* was expressed in the endodermis under standard growth conditions (22 °C). RT-PCR analysis of *CBF3* expression in *blj jkd scr* detected downregulation (Fig. 4D), indicating that this gene is functionally under the control of BLJ, JKD and SCR.

To investigate if CBF3 may regulate stem cell niche functionality, we analyzed *cbf3* loss of function mutant and *35S::CBF3* overexpressing line. We observed altered organization of the stem cell niche in *cbf3* with increased number of QC cells (penetrance 35 %) and stem niche disorganization. In contrast, *35S::CBF3* stem niche always looked well organized resembling stem cell niches at earlier developmental stages with reduced number of QC cells (Fig. 4E). To assess the functional stem cell niche state, we studied WOX5 expression within the QC. We observed decrease expression of WOX5 in *cbf3* plants (along with QC disorganization) while overexpressing *CBF3* resulted in greater expression levels in comparison with WT plants (Fig. 4F).

To investigate if CBF3 could function as a signal to regulate the stem cell niche from the ground tissue, we introgressed J0571*/GAL4-UAS::CBF3::YFP* into *blj jkd scr*. We observed increased meristem size as compared to J0571 *blj jkd scr*, and notably, recovery of the radial pattern organization with primary tissue layers being recognizable, while no obvious radial pattern could be easily identified in *blj jkd scr* (Fig. 4G, H). When we introgressed the J0571*/GAL4-UAS::DAZ3* and *J0571/GAL4-UAS::NF-YB5* lines in *blj jkd scr* we observed modest or no recovery (Fig. S4C). As

bioRxiv preprint doi: https://doi.org/10.1101/803973; this version posted October 14, 2019. The copyright holder for this preprint (which was not certified by peer review) is the author/funder. All rights reserved. No reuse allowed without permission.

BLJ, JKD and SCR must regulate SHR non-cell-autonomously and CBF3 rescues most defects observed in *blj jkd scr* when expressed in the ground tissue we investigated if CBF3 could regulate SHR levels. We observed reduced SHR protein accumulation in *cbf3* mutant (Fig. S5).

Quiescent-center-mediated regeneration of stem cells requires BLUEJAY, JACKDAW and SCARECROW

Our data also showed that BLJ, JKD and SCR were required to maintain number of QC cells, suggesting that loss of tissues in *blj jkd scr* could be caused by impairment in QC-mediated regeneration of tissue stem cells or initials during development. To further investigate this hypothesis, we treated roots with bleomycin, using a concentration which specifically killed stems cells (0.8 µg/mL). After 24-hour treatment we observed reduced number of dead cells in *blj jkd scr*, suggesting that initially at 5 dpi this mutant has fewer numbers of stem cells. Notably, upon bleomycin recovery, we just detected a few divisions of QC cells in *blj jkd scr*, while QC cells in the WT divided actively as indicated by WOX5-GFP marker (Fig. 5A).

To test stem cell niche regeneration in *blj jkd scr,* we performed laser ablation of stem cells above the QC, as this procedure results in the re-specification of a new stem cell niche. Ablated cells collapsed over time forming a scar, while division of QC cells took place concomitant with specification of WOX5-GFP marked cells for first 48 hours following ablation. In *blj jkd scr*, QC cells divided less than in the WT and in addition there was a strong reduction in the number of newly specified WOX5-GFP marked cells (Fig. 5B, Fig. S6A, B). At 72 hours after ablation, WOX5-GFP expression in the WT was confined to a few cells (the new QC) within the new stem cell niche. In addition, cells more distal to the new QC and adjacent to the scar started to elongate resembling columella differentiation. Conversely, no regeneration of a new stem cell niche was observed in *blj jkd scr* meristems which degenerated (Fig. 6C).

Stem cell niche regeneration and re-establishment of the radial pattern upon laser ablation requires *CBF3* expression in the ground tissue

To determine the role of CBF3 in stem cell niche regeneration, we performed laser ablation in J0571/GAL4-UAS::CBF3::YFP introgressed into *blj jkd scr* as well as in *cbf3* and *35S::CBF3* overexpressing line. In this experiment we focused on cell morphologies and regeneration capacity. Strikingly, we detected that regeneration capacity of *blj jkd scr* expressing J0571/GAL4-UAS::CBF3::YFP occurred at similar rates as the WT, while *blj jkd scr* mutant was severely impaired as previously mentioned (Fig. 6A, B, Fig. S6C).

bioRxiv preprint doi: https://doi.org/10.1101/803973; this version posted October 14, 2019. The copyright holder for this preprint (which was not certified by peer review) is the author/funder. All rights reserved. No reuse allowed without permission.

Evaluation of regenerated stem cell niches in *blj jkd scr* J0571/GAL4-UAS::CBF3::YFP revealed absence of elongated cells adjacent to the scar as in the WT (Fig. 6A, B). Furthermore, regenerated stem cell niches of *35S::CBF3* did not normally show elongated cells either, whereas *cbf3* regenerated stem cell niches tended to have two rows of elongated cells (Fig. 6C, D). As elongation associates with cell differentiation, these results indicate that CBF3 appears to regulate the differentiation state of the stem cell niche during regeneration. Finally, we analyze the radial pattern during regeneration. We found recovery of the radial pattern in *blj jkd scr* J0571/GAL4-UAS::CBF3::YFP as compared to the WT. Taken together, these results suggest non-cell-autonomous regulation of stem cell niche regeneration and patterning by CBF3.

DISCUSSION

A non-cell-autonomous model for coordination of positional information in the root meristem

Protein movement is critical for plant development. Over last decades organ formation and differentiation have been shown to rely on mobile TFs delivering positional information. In the root meristem, SHR movement from inner vasculature to the ground tissue was shown to regulate important aspects of radial tissue organization in layers or radial patterning, such cortex/endodermis and protoxylem/metaxylem specification from daughter cells of tissue initials or their lineages (13, 14). More recently, it has been shown that SHR movement is also required for QC and stem cell niche specification (14, 18). Additional positional information to specify the QC and the stem cell niche in the longitudinal axis is delivered by auxin hormone gradient. Auxin maxima induce PLT and high PLT dose associates with stem cell niche specification (11). Based on our data, CBF3 emerges as an important component in the regulation of positional information and cell to cell communication in the root meristem. Coordination between SHR activation and movement with the auxin gradient to specify the stem cell niche-has not been previously demonstrated. Our results show that CBF3, which is in the SHR pathway, moves to the vasculature and the stem cell niche promoting auxin transport and auxin gradient formation. Changes in the levels of SHR (or its downstream targets BLJ, JKD and SCR) could, therefore, modify auxin levels through CBF3, in this way, coordinating these two pathways.

CBF3 also regulates SHR levels, as shown by less SHR in *cbf3*. How transcription of *SHR* is regulated is not well understood. Our results show that CBF3 may work as a feedback loop activating *SHR* expression levels during development, likely acting in a non-cell-autonomous manner. *CBF3* expression in the ground tissue might be activated

bioRxiv preprint doi: https://doi.org/10.1101/803973; this version posted October 14, 2019. The copyright holder for this preprint (which was not certified by peer review) is the author/funder. All rights reserved. No reuse allowed without permission.

at certain levels or threshold of SHR, SCR, JKD or BLJ to maintain SHR levels, thus likely working as a rheostat .

Non-cell-autonomous regulation of stem cell regeneration maintains the radial pattern

In our model, CBF3 emerges as a key component in the coordination and regulation of factors leading to QC and stem cell specification. The QC was originally shown to maintain surrounding stem cells active and undifferentiated (4). More recently, the QC has been shown to be able to replace damaged stem cells upon stress (31, 32) and during regular development (5). However, the functional implications of stem cell replacement by the QC in radial patterning are unclear. Our results, indicate that reduced number of QC cells with low regenerative capacities (as in *blj jkd scr* mutant) results in loss of tissue lineages. Expressing *CBF3* (*J0571 UAS::CBF3::YFP*) in *blj jkd scr* ground tissue rescues most radial pattern defects (except endodermis formation) during development and regeneration, highlighting the importance of non-cell-autonomous regulation during postembryonic development.

Regulation of genes required for stem cell niche specification and regeneration involves CBF3

SHR and its direct target JKD show a specific interaction that promotes *WOX5* activation; furthermore, increased accumulation of JKD in the QC is sufficient to induce specification of QC-like cells in the absence of SCR (20). In turn, SCR was shown to be required for QC specification and maintenance (21); although, intriguingly, SCR interaction with SHR did not appear to be relevant for *WOX5* activation (20). More recently, SCR has been shown to work in combination with PLT3 and TCP20 to activate *WOX5* expression (24). In this model of regulation, SHR and JKD on the one hand, and PLT and TCP, on the other, emerge as critical regulators of gene transcription leading to QC specification, while SCR might regulate their combinatorial interactions or work as a scaffold. In agreement with these previous results, our data show that CBF3 may promote SHR accumulation, which would lead to QC specification. In addition, we detected recovery in stem cell niche specification and complementation in the absence of JKD and SCR- (*blj jkd scr* mutant), suggesting that an increase in SHR levels might compensate for absence of these two factors. In addition, as SHR is barely nuclear localized in the absence of JKD and SCR (18) it is possible that CBF3 or a downstream target might also target SHR to QC nuclei. An alternative hypothesis might involve CBF3 directly binding to genes involved in QC specification and regeneration to activate their transcription.

bioRxiv preprint doi: https://doi.org/10.1101/803973; this version posted October 14, 2019. The copyright holder for this preprint (which was not certified by peer review) is the author/funder. All rights reserved. No reuse allowed without permission.

Future perspectives

Pattern restoration upon cell-type targeted ablation or wounding has been shown to involve SHR and PLT triggering formative divisions in inner adjacent cells (29). As SHR moves from inside to outside, signaling and activation of regenerative divisions (from wounded cells) might require the existence of unknown positional signaling. Our data show that *CBF3* expression in the ground tissue (which moves from outside to inside) is sufficient to restore stem cell regeneration upon ablation of specific vasculature cells. Future research might reveal a role for CBF3 as a signal delivering positional information required for cell fate specification upon wounding.

MATERIALS AND METHODS

Growth Conditions

Seeds were sterilized in 25% (m/v) NaClO and rinsed three times with sterile water before being sowed on 120 × 120 × 10 mm petri dishes containing 65 mL of one-half-Murashige & Skoog (MS) medium with 1% Sucrose and 10 g/L Plant Agar (Duchefa). For all the experiments, after 2 days of stratification at 4°C in darkness, plates were transferred to a custom made growth chamber and maintained vertically at 22°C with 16/8 hours light/darkness photoperiod at a white light rate intensity of 50 $\mu mol \cdot m^{-2} \cdot s^{-1}$. For bleomycin treatment, seeds were sown on MS medium with 0.8 µg/mL or 1.5 µg/ml bleomycin sulfate (Calbiochem) as indicated. For aluminium chloride treatment, 6 days-after-imbibition seedlings were transferred to moistened 3MM paper located on sides of magenta boxes containing 50 mL of 300 µM $AlCl_3$ or distilled water as mock and cultured in growth chamber under previously described conditions.

Generation of constructs

For generation of pCBF3:NLS:3xmCherry line, a fragment of 2776 bp upstream of *CBF3* start codon was amplified by PCR (Phusion High-Fidelity DNA Polymerase Thermo Fisher Scientific) using F 5´-ACTTCTTTGCTTCACATAAGTTAAAAGTCA-3´and R 5´-TCTTGAAACAGAGTACTCTTCTGATCA-3´ primers from *A. thaliana* (Col-0) genomic DNA. The fragment was cloned into pNYZ28-A (NYZ tech) and P4P1R entry vector. For generation of UAS constructs, the UAS promoter (21) was cloned into P4P1R entry vector and coding sequences amplified by PCR with primers *CBF3*-At4g25480 F 5´-CACCATGAACTCATTTTCTGCTTTTTC-3' and R 5'-ATAACTCCATAACGATACGTCG-3', NF-YB5-AT2G47810 F 5'-CACCATGGCGGGGAATTATCATTCG-3' and R 5'-ATTATCTGGCGAGGATTTAGG-3' , BHLH114/E29 (At4g05170) F 5'-CACCATGAACATGCATAATAGTTTCTTC-3' and R 5'-CAAAGAATGGAAGATGCCAGA-3', BHLH103/B70/E30 (At4g21340) F5'-

bioRxiv preprint doi: https://doi.org/10.1101/803973; this version posted October 14, 2019. The copyright holder for this preprint (which was not certified by peer review) is the author/funder. All rights reserved. No reuse allowed without permission.

CACCATGACAGAAGAATTCGACACTA-3' and R 5'-ATTCCACAAACTAGATGTGTC-3' and DAZ3 (At4g35700) 5'-CACCATGAGTAATCCCGAGAAGTCT-3' and R 5'-CTCGACTTTATCATCGTTCTC-3' and cDNA as template and introduced into pD-TOPO entry vector. Final constructs into dpGreenBarT vector were generated using 3-fragment GATEWAY System (Thermo Fisher Scientific) and transformed into Col-0 or J0571 as indicated using floral dipping method.

Plant Material

Columbia-0 (Col-0) and Wassilewskija-2 (Ws-2) accessions were used as a genetic background as corresponding. The reporter lines pCYCB1;1:CYCB1;1:GFP (37), *shr2* pSHR2:SHR2:GFP (38), pPLT2:PLT2:eYFP (11), pPIN1:PIN1:GFP (39), pPIN4:PIN4:GFP (40), pDR5:NLS:eYFP (39), pSMB3:SMB3:GFP (41), pWOX5:ER:GFP (33), pWER:ER:GFP (42), pWOL:ER:GFP (43) were introgressed by crossing into *blj jkd-4 scr-4* (15), *cbf3-1* (SAIL_244_D02 from NASC) and OX CBF3 A30 (CS69502 from NASC). OX CBF A30 was crossed to pPLT2:PLT2:eYFP and *shr2* pSHR:SHR:GFP and examined in F1 generation. UAS::CBF3-YFP J0571 was introgressed by crossing into *blj jkd-4 scr-4* J0571 line (15). Transgenic line *shr2 plt1 plt2* (44) was also used in this work.

Genotyping

DNA extraction from F2 seedlings was used for genotyping by PCR using the following oligonucleotides: *blj* F 5´- CTTGAATCTCAAGCAGAAGCG-3´and R 5´-TCTTGGTTTCTTCTCTGCATCTC-3´; *jkd-4* F 5´- GGATGAAAGCAATGCAAAACA-3´ and R 5´- AATGTCGGGATGATGAACTCC-3´; *scr-4* F 5´-TTATCCATTCCTCAACTTCAGT -3´and R 5´- TGGTGCATCGGTAGAAGAATT-3´ and *cbf3-1* F 5´- AGTCTTCTCTGGACACATGGC-3´ and R 5´-TCCATAACGATACGTCGTCATC-3´. T-DNA insertions were genotyped using the following pairs of primers: *blj* F 5´-CTTGAATCTCAAGCAGAAGCG-3´and R 5´-ACCCGACCGGATCGTATCGGT-3´; *jkd-4* F 5´- GGATGAAAGCAATGCAAAACA-3´ and R 5´- TCAAACAGGATTTTCGCCTGCT-3´; *cbf3-1* F 5´-AGTCTTCTCTGGACACATGGC-3´ and R 5´-TAGCATCTGAATTTCATAACCAATCTCGATACA C-3´. Mutation in *scr-4* was genotyped by using the primers F 5´- CTTATCCATTCCTCAACTCTATT-3´and R 5´-TGGTGCATCGGTAGAAGAATT-3´ while absence of *scr-4* mutation was detected using F 5´- TTATCCATTCCTCAACTTCAGT -3´and R 5´-TGGTGCATCGGTAGAAGAATT-3´.

Microscopy analysis.

bioRxiv preprint doi: https://doi.org/10.1101/803973; this version posted October 14, 2019. The copyright holder for this preprint (which was not certified by peer review) is the author/funder. All rights reserved. No reuse allowed without permission.

Roots were stained with propidium iodide (10mg/mL. Sigma-Aldrich) and imaged using a TCS SP8 confocal microscope (Leica). Mature embryos were stained using the aniline blue staining method and scanned by confocal microscopy as described by (45). Laser ablation of specific cells was performed with one to three pulses of 30 seconds with a UV laser (405nm) using FRAP mode of TCS SP8. Root meristem size measurements were performed as described by (21) using Image J program (Bethesda, MD, USA). Division of quiescent center (QC) cells upon laser ablation recovery was determined through confocal microscopy imaging of 1.5µm sections of the whole stem cell niche every 24 hours and scored as the number of QC cells generated by division of QC cells marked with pWOX:ER:GFP in the same root. pWOX5 marked cells was scored as the number of pWOX5:ER:GFP marked cells outside of QC using the same imaging approach.

Real time quantitative polymerase chain reaction (RT-qPCR) analysis.

Root meristems were dissected at 6 day after imbibition using a micro scalpel (MICRO FEATHER) under a stereo microscope (Leica MZ95). RNA was isolated with the RNeasy isolation kit (Quiagen) and RNA integrity was measured with pico chip Bioanalyzer 2100. cDNA synthesis was performed with NYZ First-Strand cDNA Synthesis Kit (NYZ tech). RT-qPCR was performed in ECO Real-Time PCR System (Illumina) with MasterMix qPCR ROx PyroTaq EvaGreen dye (CMB) with ROX inner normalization. The following pairs of primers were used: AT3G07730 F 5´-TTGTTGTTGGATGGCAATCTG-3´and R 5´- AGTCTTGAGACATTGCATCAGT-3´ as control and *CBF3* F 5´- CAGTTTCAGTATAAGTGTGGGC-3´and R 5´-GCTGAATCGGTTGTTTCGGT-3´.

Data collection and Statistical Analysis

For laser ablation experiments, at least 20 roots were assayed for each genetic background in two independent rounds. For root growth, meristem size and meristem differentiation measurements 60-90 seedlings of each genetic background in 2-3 independent rounds were used. SPSS Statistics 21 software (IBM) was used for statistical analysis. Normality and variance distributions were assayed using Kolmogorov-Smirnov and Levene tests, respectively. Significance in distributions of means was performed by General Linear Model (GLM) to assess for differences between genotypes, or when genotypes were compared at specific times, with a least significant difference (LSD) posthoc test. ANOVA was used to asses for differences when samples to compare were <3, as indicated.

bioRxiv preprint doi: https://doi.org/10.1101/803973; this version posted October 14, 2019. The copyright holder for this preprint (which was not certified by peer review) is the author/funder. All rights reserved. No reuse allowed without permission.

Microarray analysis

Microarrays correspond to reference GSE60157. Normalization and differentially expressed genes were calculated as previously described (15, 46), comparing set of microarrays only processed with the same Affymetrix kit and using the follwing cut-off settings: fold-change >±1.5, q-value < 10E-3 and expression value >1.

Identification of transcription factors with enriched expression in the ground tissue

For identification of transcription factors with enriched expression in the ground tissue, Arabidopsis transcription factors in database PlantTFDB 3.0 (47) were required to be expressed in the ground tissue (J0571 cell type>1) and not be expressed (<1) in root-hair cells (COBL9 cell type), hairless cells (GL2 cell types), lateral root cap (J3411 cell type) nor columella (PET111 cell type) of the RootMap (48). In addition, they were required to: a) not be expressed (<1) in the quiescent center (AGL42 cell type) nor the stele (WOL cell type) or b) be at least 2-fold-enriched in the ground tissue (J0571) in comparison with the quiescent center (AGL2) and the mean value of the cell types which make up the stele (J2661, JO121-pericycle, APL, S32-phloem, SUC2-companion cells, J2501, S4, S18-xylem). Intersection of all criteria to identify candidate genes was performed in Microsoft Access.

ACKNOWLEDGMENTS

This work was supported by grants from Ministerio de Economía y Competitividad (MINECO) of Spain and ERDF BFU2013-41160-P and BFU2016-80315-P to M.A.M.-R. A.S.-C. was supported by a FPI contract from MINECO. P.P.-G. was supported by a Juan de la Cierva contract from MINECO and Programa Atraccion Talento from Comunidad Madrid. J.C was supported by a Juan de la Cierva contract from MINECO.

REFERENCES

1. Perez-Garcia P & Moreno-Risueno MA (2018) Stem cells and plant regeneration. *Developmental Biology* 442(1):3-12.
2. Dinneny JR & Benfey PN (2008) Plant Stem Cell Niches: Standing the Test of Time. *Cell* 132(4):553-557.
3. Pierre-Jerome E, Drapek C, & Benfey PN (2018) Regulation of Division and Differentiation of Plant Stem Cells. *Annual Review of Cell and Developmental Biology* 34(1):289-310.
4. Sarkar AK, *et al.* (2007) Conserved factors regulate signalling in Arabidopsis thaliana shoot and root stem cell organizers. *Nature* 446(7137):811.

bioRxiv preprint doi: https://doi.org/10.1101/803973; this version posted October 14, 2019. The copyright holder for this preprint (which was not certified by peer review) is the author/funder. All rights reserved. No reuse allowed without permission.

5. Cruz-Ramírez A, *et al.* (2013) A SCARECROW-RETINOBLASTOMA Protein Network Controls Protective Quiescence in the Arabidopsis Root Stem Cell Organizer. *PLoS Biology* 11(11):e1001724.
6. Greb T & Lohmann JU (2016) Plant stem cells. *Current biology* 26(17):R816-R821.
7. Sabatini S (2003) SCARECROW is involved in positioning the stem cell niche in the Arabidopsis root meristem. *Genes & Development* 17(3):354-358.
8. Galinha C, *et al.* (2007) PLETHORA proteins as dose-dependent master regulators of Arabidopsis root development. *Nature* 449(7165):1053-1057.
9. Aida M, *et al.* (2004) The PLETHORA Genes Mediate Patterning of the Arabidopsis Root Stem Cell Niche. *Cell* 119(1):109-120.
10. Grieneisen VA, Xu J, Marée AFM, Hogeweg P, & Scheres B (2007) Auxin transport is sufficient to generate a maximum and gradient guiding root growth. *Nature* 449(7165):1008-1013.
11. Mähönen AP, *et al.* (2014) PLETHORA gradient formation mechanism separates auxin responses. *Nature* 515(7525):125.
12. Santuari L, *et al.* (2016) The PLETHORA Gene Regulatory Network Guides Growth and Cell Differentiation in Arabidopsis Roots. *The Plant Cell* 28(12):2937-2951.
13. Helariutta Y, *et al.* (2000) The SHORT-ROOT gene controls radial patterning of the Arabidopsis root through radial signaling. *Cell* 101(5):555-567.
14. Nakajima K, Sena G, Nawy T, & Benfey PN (2001) Intercellular movement of the putative transcription factor SHR in root patterning. *Nature* 413(6853):307-311.
15. Moreno-Risueno MA, *et al.* (2015) Transcriptional control of tissue formation throughout root development. *Science* 350(6259):426-430.
16. Koizumi K, Hayashi T, Wu S, & Gallagher KL (2012) The SHORT-ROOT protein acts as a mobile, dose-dependent signal in patterning the ground tissue. *Proceedings of the National Academy of Sciences* 109(32):13010-13015.
17. Cui H, *et al.* (2007) An Evolutionarily Conserved Mechanism Delimiting SHR Movement Defines a Single Layer of Endodermis in Plants. *Science* 316(5823):421-425.
18. Long Y, *et al.* (2015) Arabidopsis BIRD zinc finger proteins jointly stabilize tissue boundaries by confining the cell fate regulator SHORT-ROOT and contributing to fate specification. *The Plant Cell* 27(4):1185-1199.
19. Di Mambro R, Sabatini S, & Dello Ioio R (2018) Patterning the Axes: A Lesson from the Root. *Plants* 8(1):8.
20. Long Y, *et al.* (2017) In vivo FRET–FLIM reveals cell-type-specific protein interactions in Arabidopsis roots. *Nature* 548(7665):97-102.
21. Sabatini S, Heidstra R, Wildwater M, & Scheres B (2003) SCARECROW is involved in positioning the stem cell niche in the Arabidopsis root meristem. *Genes & development* 17(3):354-358.
22. Moubayidin L, *et al.* (2016) A SCARECROW-based regulatory circuit controls Arabidopsis thaliana meristem size from the root endodermis. *Planta* 243(5):1159-1168.
23. Moubayidin L, *et al.* (2013) Spatial Coordination between Stem Cell Activity and Cell Differentiation in the Root Meristem. *Developmental Cell* 26(4):405-415.
24. Shimotohno A, Heidstra R, Blilou I, & Scheres B (2018) Root stem cell niche organizer specification by molecular convergence of PLETHORA and SCARECROW transcription factor modules. *Genes & Development* 32(15-16):1085-1100.
25. Stahl Y, Wink RH, Ingram GC, & Simon R (2009) A Signaling Module Controlling the Stem Cell Niche in Arabidopsis Root Meristems. *Current Biology* 19(11):909-914.
26. Zhang Y, Jiao Y, Liu Z, & Zhu Y-X (2015) ROW1 maintains quiescent centre identity by confining WOX5 expression to specific cells. *Nature Communications* 6(1).

bioRxiv preprint doi: https://doi.org/10.1101/803973; this version posted October 14, 2019. The copyright holder for this preprint (which was not certified by peer review) is the author/funder. All rights reserved. No reuse allowed without permission.

27. Pi L, *et al.* (2015) Organizer-derived WOX5 signal maintains root columella stem cells through chromatin-mediated repression of CDF4 expression. *Developmental cell* 33(5):576-588.
28. Efroni I, *et al.* (2016) Root regeneration triggers an embryo-like sequence guided by hormonal interactions. *Cell* 165(7):1721-1733.
29. Marhava P, *et al.* (2019) Re-activation of Stem Cell Pathways for Pattern Restoration in Plant Wound Healing. *Cell* 177(4):957-969.e913.
30. Forzani C, *et al.* (2014) WOX5 Suppresses CYCLIN D Activity to Establish Quiescence at the Center of the Root Stem Cell Niche. *Current Biology* 24(16):1939-1944.
31. Fulcher N & Sablowski R (2009) Hypersensitivity to DNA damage in plant stem cell niches. *Proceedings of the National Academy of Sciences* 106(49):20984-20988.
32. Heyman J, *et al.* (2013) ERF115 controls root quiescent center cell division and stem cell replenishment. *Science* 342(6160):860-863.
33. Xu J (2006) A Molecular Framework for Plant Regeneration. *Science* 311(5759):385-388.
34. Silva-Navas J, *et al.* (2016) Flavonols Mediate Root Phototropism and Growth through Regulation of Proliferation-to-Differentiation Transition. *The Plant Cell* 28(6):1372-1387.
35. Friml J, *et al.* (2002) AtPIN4 mediates sink-driven auxin gradients and root patterning in Arabidopsis. *Cell* 108(5):661-673.
36. Zhou M, Chen H, Wei D, Ma H, & Lin J (2017) Arabidopsis CBF3 and DELLAs positively regulate each other in response to low temperature. *Scientific Reports* 7(1).
37. Weingartner M (2004) Expression of a Nondegradable Cyclin B1 Affects Plant Development and Leads to Endomitosis by Inhibiting the Formation of a Phragmoplast. *The Plant Cell Online* 16(3):643-657.
38. Sozzani R, *et al.* (2010) Spatiotemporal regulation of cell-cycle genes by SHORTROOT links patterning and growth. *Nature* 466(7302):128-132.
39. Heisler MG, *et al.* (2005) Patterns of Auxin Transport and Gene Expression during Primordium Development Revealed by Live Imaging of the Arabidopsis Inflorescence Meristem. *Current Biology* 15(21):1899-1911.
40. Vieten A, *et al.* (2005) Functional redundancy of PIN proteins is accompanied by auxin-dependentcross-regulation of PIN expression. *Development* 132(20):4521-4531.
41. Willemsen V, *et al.* (2008) The NAC domain transcription factors FEZ and SOMBRERO control the orientation of cell division plane in Arabidopsis root stem cells. *Developmental cell* 15(6):913-922.
42. Lee MM & Schiefelbein J (1999) WEREWOLF, a MYB-related protein in Arabidopsis, is a position-dependent regulator of epidermal cell patterning. *Cell* 99(5):473-483.
43. Mahonen AP, *et al.* (2000) A novel two-component hybrid molecule regulates vascular morphogenesis of the Arabidopsis root. *Genes Dev* 14(23):2938-2943.
44. Bustillo-Avendaño E, *et al.* (2017) Regulation of Hormonal Control, Cell Reprogramming and Patterning during De Novo Root Organogenesis. *Plant physiology*:pp. 00980.02017.
45. Bougourd S, Marrison J, & Haseloff J (2000) Technical advance: an aniline blue staining procedure for confocal microscopy and 3D imaging of normal and perturbed cellular phenotypes in mature Arabidopsis embryos. *The Plant journal : for cell and molecular biology* 24(4):543-550.
46. Levesque MP, *et al.* (2006) Whole-Genome Analysis of the SHORT-ROOT Developmental Pathway in Arabidopsis. *PLoS Biology* 4(5):e143.
47. Jin J, *et al.* (2017) PlantTFDB 4.0: toward a central hub for transcription factors and regulatory interactions in plants. *Nucleic Acids Research* 45(D1):D1040-D1045.
48. Brady SM, *et al.* (2007) A High-Resolution Root Spatiotemporal Map Reveals Dominant Expression Patterns. *Science* 318(5851):801-806.

bioRxiv preprint doi: https://doi.org/10.1101/803973; this version posted October 14, 2019. The copyright holder for this preprint (which was not certified by peer review) is the author/funder. All rights reserved. No reuse allowed without permission.

FIGURE LEGENDS

Fig. 1. BLUEJAY, JACKDAW and SCARECROW work combinedly to maintain the Arabidopsis root meristem and the radial pattern. A, seedling images of the wild type (WT) and of combinations of *jackdaw-4* (*jkd4)*, *scarecrow-4 (scr4)* and *bluejay (blj)* mutants at 10 days post imbibition (dpi). **B**, quantification of radial patterns alterations in WT, *scr4*, *jkd4 scr4* and *blj jkd4 scr4* plants at 8 dpi. **C**, Confocal images showing representative radial patterns of WT, *scr4*, *jkd4 scr4* and *blj jkd4 scr4* plants at 8 dpi. **D,** confocal cross-sections of WT and *blj jkd4 scr4* RAMs at 13 dpi**.** Scale bar: 0.25 µm. Yellow dotted line: boundary between vascular and external tissues. Green dotted line: abnormal organization of cells in rows. **E,** percentage of differentiation-related or meristematic-related genes repressed or activated in microarrays of the RAM of *blj jkd4 scr4*. **F,** percentage of RAMs showing root hairs (differentiation) in WT, *shr2*, *scr4*, *jkd4 scr4*, *plt1 plt2*, *blj jkd4 scr4* and *shr2 plt1 plt2*.

Fig. 2. Root stem cell niche functionality is affected in the absence of BLUEJAY, JACKDAW and SCARECROW. A, confocal images showing the expression of *pSMB3:SMB3:GFP* differentiated columella and lateral root cap cell lineage marker in WT and *blj jkd4 scr4* at 6dpi. White asterisk: Quiescent cells. Inset: close-up image of the stem cell niche. **B**, Confocal images showing expression of *pWOX5:ER:GFP* quiescent cells lineage marker in WT and *blj jkd4 scr4* at 6dpi. White arrowhead: Quiescent cells. **C**, Confocal images showing expression of *pWOX5:ER:GFP* quiescent cells lineage marker in WT at 7dpi, at 5 dpi after treatment with bleomycin and after 48 hours of recovery. White arrowhead: Non-damage quiescent cells. **D**, Confocal image of *blj jkd4 scr4* triple mutant at 12 dpi. Scale bars: 25 µm.

Fig. 3. Vascular expressed regulators are regulated by BLUEJAY, JACKDAW and SCARECROW. A, Confocal images showing the accumulation of *pSHR:SHR:GFP* in WT and *blj jkd4 scrc4* plants at 6dpi. Graph comparing the accumulation of *pSHR:SHR:GFP* in WT and *blj jkd4 scrc4* plants at 6dpi. **B**, Confocal images showing the accumulation of *pPIN1:PIN1:GFP* in WT and *blj jkd4 scrc4* plants at 6dpi. Graph comparing the accumulation of *pPIN1:PIN1:GFP* in WT and *blj jkd4 scrc4* plants at 6dpi. **C**, Confocal images showing the accumulation of *pPIN4:PIN4:GFP* in WT and *blj jkd4 scrc4* plants at 6dpi. Graph comparing the accumulation of *pPIN4:PIN4:GFP* in WT and *blj jkd4 scrc4* plants at 6dpi. **D**, Confocal images showing the expression of *pDR5:NLS:YFP* in WT and *blj jkd4 scrc4* plants at 6dpi. Graph comparing the expression of *pDR5:NLS:YFP* in WT and *blj jkd4 scrc4* plants at 6dpi. Scale bars; 25 µm. Asterisk: p-value<0.001 in a one-way ANOVA. MIV/pixel: mean intensity value/pixel.

bioRxiv preprint doi: https://doi.org/10.1101/803973; this version posted October 14, 2019. The copyright holder for this preprint (which was not certified by peer review) is the author/funder. All rights reserved. No reuse allowed without permission.

Fig. 4. C REPEAT BINDING FACTOR 3 (CBF3) moves out from the ground tissue and regulates stem cell niche differentiation and root radial pattern. A, venn diagram. **B**, confocal images showing localization of yellow fluorescet protein (YFP)-tagged CBF3 in the UAS/GAL4 system and enhancer trap line J0571, which drives expression to the ground tissue (GFP marked). Blue arrows: ectopics divisions in ground tissue. **C**, CBF3 promoter expression in the RAM. Yellow arrowheads: nuclear loalized mCherry fluorescent protein under the control of CBF3 promoter. **D**, Real-time PCR analysis of CBF3 expression in WT and *blj jkd4 scr4* RAMs at 6 dpi. Cross: p-valu<0.05 in a one-way ANOVA. **E**, confocal images of the stem cell niche of WT, cbf3-1 and p35S:CBF3 at 9dpi. **F**, Confocal images showing the expression of *pWOX5:ER:GFP* in WT, cbf3-1 and p35S:CBF3 plants at 9dpi. Graph comparing the expression of *pWOX5:ER:GFP* in WT and *blj jkd4 scrc4* plants at 9dpi. **G**, confocal images at 9 dpi of the RAM of *blj jkd4 scr4* J0571 and *UAS:CBF3:eYFP* introgressed into *blj jkd4 scr4* J0571. Lrc: lateral root cap, e: epidermis, gt: ground tissue, v:vasculature. Green arrowheads: end of the meristem. H, Meristem size of *blj jkd4 scr4* J0571 and *UAS:CBF3:eYFP* at 9dpi. Asterisk: p-value<0,001 in a one-way ANOVA. MIV/pixel: mean intensity value/pixel. Scale bars: 25 µm.

Fig. 5. BLUEJAY, JACKDAW *and* SCARECROW are required for quiescent center mediated regeneration and stem cell niche formation. A, confocal 48-hours (h)-time-lapse images of stem cell niche regeneration upon low dose of bleomycin treatment (0.8 ug/mL). WT and *blj jkd4 scr4* roots carrying the *pWOX5:ER:GFP* QC marker were treated for 24h and then moved to bleomycin-free medium to asses recovery. **B-C**, confocal 72h-time-lapse images of stem cell niche regeneration upon laser ablation of stem cells above the QC, in WT and *blj jkd4 scr4* roots carrying the *pWOX5:ER:GFP* QC marker. AC: ablated cells. Dashed line: elongated cells (twice the size than adjacent upper cells). White arrow: follow-up during regeneration of an adjacent cell lower to QC at the time of ablation. Scale bars: 25 µm.

Fig. 6. CBF3 regulates stem cell niche specification and root patterning during regeneration. **A-D**, confocal images of stem cell niche regeneration upon laser ablation of cells above the QC, in WT, *blj jkd4 scr4*, *blj jkd4 scr4* J0571 *pUAS:CBF3:eYFP, cbf3-1* and *35S::CBF3* seedlings at 0 and 72h after laser ablation. AC: ablated cells. Dashed line: elongated cells (twice the size than adjacent upper cells). **E**, confocal images of root cross-sections above the QC at 48h after ablation. lrc: lateral root cap, e: epidermis, gt: ground tissue, v: vasculature. Dashed yellow line: contour delimiting the ground tissue. Scale bars: 25 µm.

bioRxiv preprint doi: https://doi.org/10.1101/803973; this version posted October 14, 2019. The copyright holder for this preprint (which was not certified by peer review) is the author/funder. All rights reserved. No reuse allowed without permission.

SUPPORTING INFORMATION

Fig. S1. BLUEJAY, JACKDAW and SCARECROW maintain root growth capacity and meristem function. A, images of *shr2*, *plt1 plt2*, *shr2 plt1 plt2* and *blj jkd4 scr4* seedlings at 10 dpi. Scale bars: 0.3 cm. **B**, root growth per day of WT, *scr4*, *blj jkd4*, *blj jkd4 scr4*, *plt1 plt2* and *shr plt1 plt2 seedlings*. mm: millimeters. **C**, confocal images of WT and *blj jkd4 scr4* mature embryos stained with aniline blue. Scale bar: 10 µm. **D**, meristem length of WT, *scr4*, *blj jkd4*, *jkd4 scr4*, *blj jkd4 scr4*, *plt1 plt2* and *shr plt1 plt2* throughout development. Asterisk: statistically significant (p-value < 0.001) by GLM and LSD post-hoc test. **E,** confocal images of the RAM of sc*r4*, *blj jkd4*, *blj jkd4 scr4*, *plethora* (*plt)1 plt2* and *short-root-2* (*shr2) plt1 plt2*. Crosses and asterisks: statistically significant (p-value < 0.05 and < 0.001, respectively) by General Linear Model (GLM) and LSD post-hoc test as compared to the WT. a and b: statistically different (p-value < 0.05) when genotypes were compared separately for each day by GLM followed by LSD. Only differences between *blj jkd4 scr4* and *plt1 plt2* are indicated. White arrowheads indicate the end of the RAM. scale bars: 25 µm.

Fig. S2. BLUEJAY, JACKDAW *and* SCARECROW regulate proliferation and differentiation programs. **A**, box plot representation of microarray means expression values for cell cycle genes in the root apical meristem (RAM) of WT and *blj jkd4 scr4*. **B,** confocal images showing the maximum projection of *pCYCB1;1::CYCB1;1::GreenFluorescentProtein (GFP)* expression in WT and *blj jkd4 scr4* RAMs at 7 dpi. Cell walls, in red (stained with propidium iodide -PI) are shown at the medium plane of the RAM. **C-D**, box-plot representations of mean-normalized expression values of **C,** repressed and **D,** activated genes in microarray experiments profiling the RAM of *blj jkd4 scr4* as compared to the WT. Expression values in the RAM of *blj jkd4 scr4* and the WT, and in rest of root developmental zones of the WT are shown for comparison.

Fig. S3. Expression levels of *SHR* and *PIN1*, *2* and *4* auxin transporter genes are repressed in meristems of *blj jkd4 scr4 triple mutant.* A-B, graphs showing microarray mean expression values of *SHR*, *PINFORMED 1*(*PIN1*), *PIN2* and *PIN2* genes in the RAM of WT and *blj jkd4 scr4*. p-values as indicated by mixed-model ANOVA of replicates.

Fig. S4. Involvement of mobile factors DUO1-ACTIVATED ZINC FINGER 3 (DAZ3) and NUCLEAR FACTOR SUBUNIT B5 (NF-YB5) NF-YB5 in maintenance of meristematic function. **A-B**, confocal images showing localization of YFP-tagged DAZ3 and NF-YB5 in the *UAS/GAL4* system and enhancer trap line J0571 at 6 dpi.

bioRxiv preprint doi: https://doi.org/10.1101/803973; this version posted October 14, 2019. The copyright holder for this preprint (which was not certified by peer review) is the author/funder. All rights reserved. No reuse allowed without permission.

Expression of transgenes under *UAS* promoter in the J0571 line corresponds to the ground tissue as indicated by localization of the GFP. **C**, confocal images of the RAM of *blj jkd4 scr4* J0571, *blj jkd4 scr4* J0571 *UAS::DAZ3::YFP* and *blj jkd4 scr4* J0571 *UAS::NF-YB5::YFP* at 12 dpi. Scale bar: 25µm.

Fig. S5. CBF3 regulates SHR protein levels. confocal images of *pSHR:SHR-GFP* in the RAM of WT and *cbf3-1* at 6 dpi. Graph comparing the accumulation of *pSHR:SHR-GFP* in the RAM of WT and *cbf3-1* at 6 dpi. MIV/pixel: mean intensity value/pixel. Scale bars: 25 µm.

Fig. S6. BLUEJAY, JACKDAW, SCARECROW and CBF3 regulate stem cell niche and root regeneration. **A**, graph showing incremental number of QC cells in WT and *blj jkd4 scr4* at 24h after laser ablation of stem cells above the QC. **B**, graph showing number of WOX5-marked cells in the 3-D root meristem volume at 24 and 48h after stem cell ablation in WT and *blj jkd4 scr4*. **C**, graph showing percentage of regeneration following laser ablation in WT, *blj jkd4 scr4* J0571 and *blj jkd4 scr4* J0571 complemented with *UAS::CBF3::YFP*. Asterisk: p-value < 0.001 by GLM and LSD post-hoc test.

bioRxiv preprint doi: https://doi.org/10.1101/803973; this version posted October 14, 2019. The copyright holder for this preprint (which was not certified by peer review) is the author/funder. All rights reserved. No reuse allowed without permission.

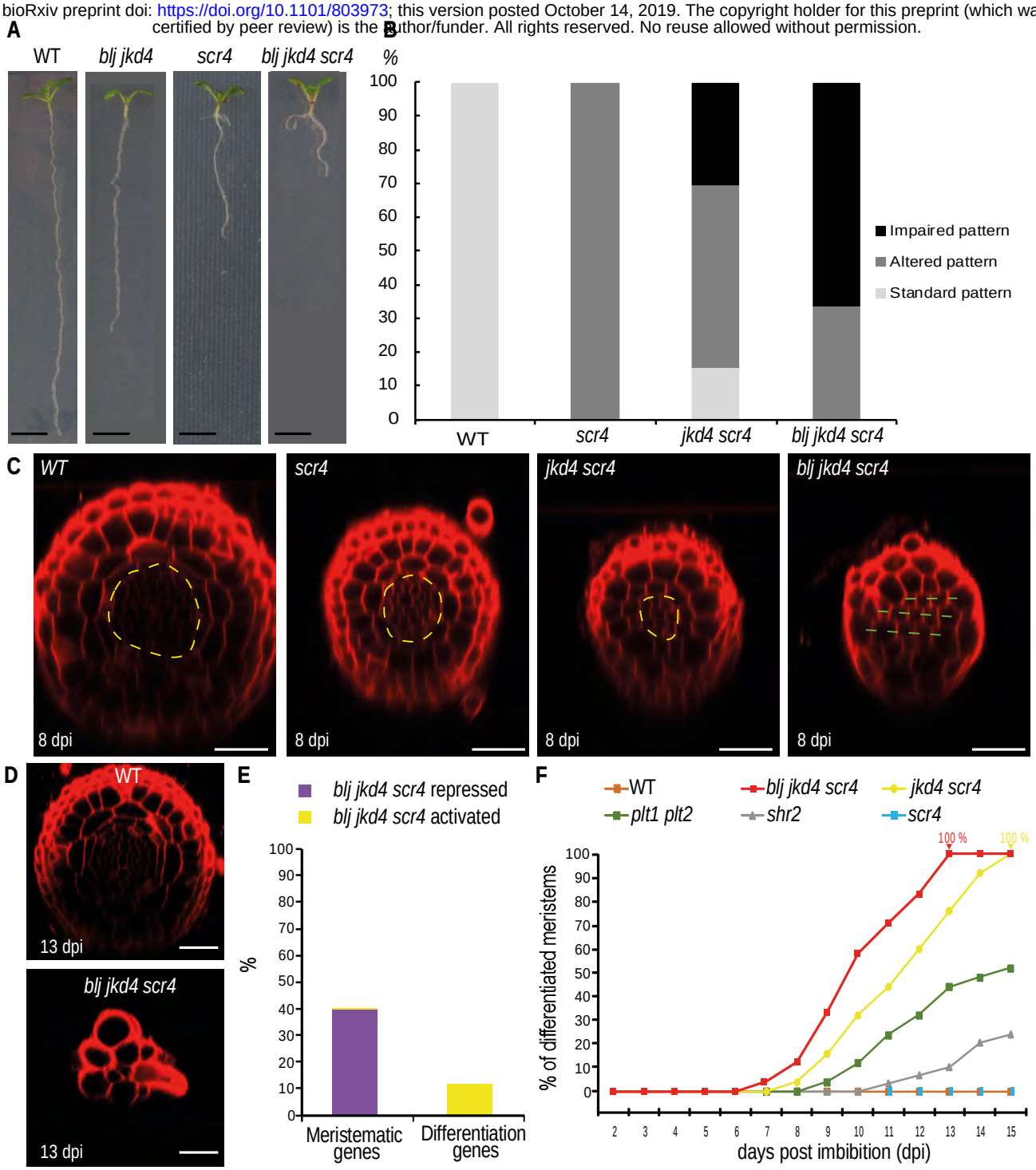

Fig. 1. BLUEJAY, JACKDAW and SCARECROW work combinedly to maintain the Arabidopsis root meristem and the radial pattern. A, seedling images of the wild type (WT) and of combinations of *jackdaw-4* (*jkd4*), *scarecrow-4 (scr4)* and *bluejay (blj)* mutants at 10 days post imbibition (dpi). **B**, quantification of radial patterns alterations in WT, *scr4*, *jkd4 scr4* and *blj jkd4 scr4* plants at 8 dpi. **C**, Confocal images showing representative radial patterns of WT, *scr4*, *jkd4 scr4* and *blj jkd4 scr4* plants at 8 dpi. **D,** confocal cross-sections of WT and *blj jkd4 scr4* RAMs at 13 dpi**.** Scale bar: 0.25 µm. Yellow dotted line: boundary between vascular and external tissues. Green dotted line: abnormal organization of cells in rows. **E,** percentage of differentiation-related or meristematic-related genes repressed or activated in microarrays of the RAM of *blj jkd4 scr4*. **F,** percentage of RAMs showing root hairs (differentiation) in WT, *shr2*, *scr4*, *jkd4 scr4*, *plt1 plt2*, *blj jkd4 scr4* and *shr2 plt1 plt2*.

bioRxiv preprint doi: https://doi.org/10.1101/808973 This version posted October 21, 2019 in the public domain. Author for this preprint (which was not certified by peer review) is the author/funder. All rights reserved. Cover art is not to be reproduced or used without permission.

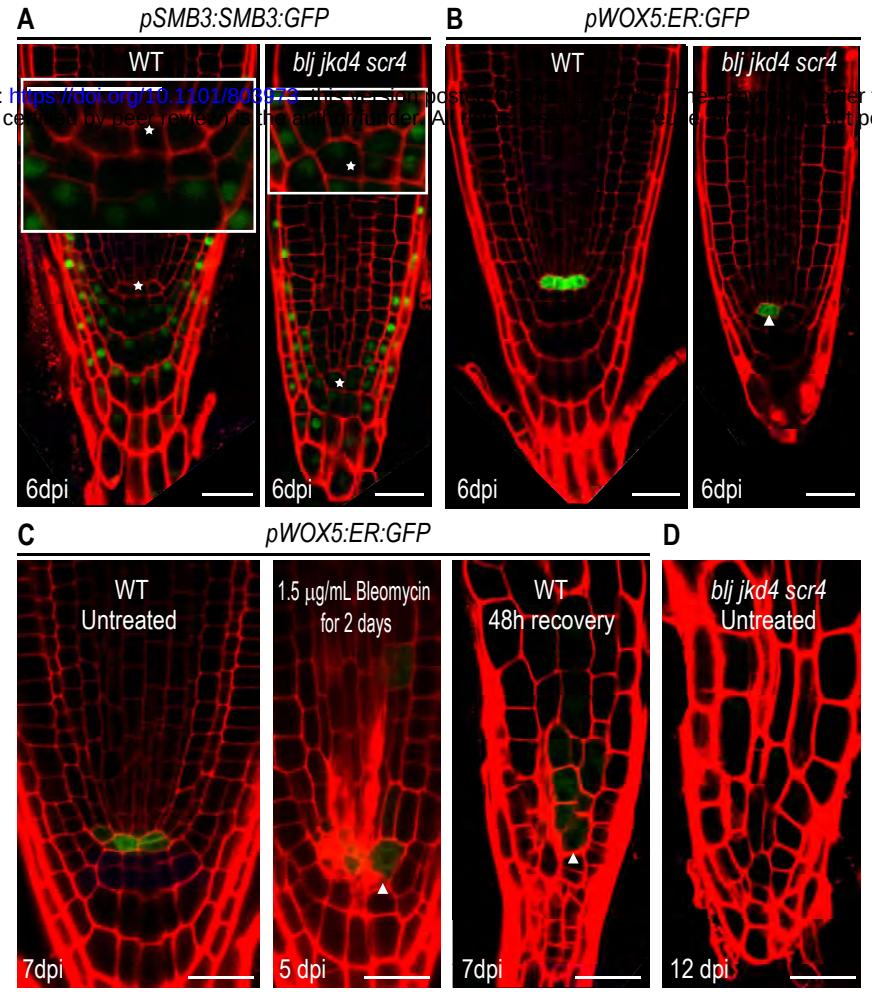

Fig. 2. Root stem cell niche functionality is affected in the absence of BLUEJAY, JACKDAW and SCARECROW. A, confocal images showing the expression of pSMB3:SMB3:GFP differentiated columella and lateral root cap cell lineage marker in WT and blj jkd4 scr4 at 6dpi. White asterisk: Quiescent cells. Inset: close-up image of the stem cell niche. **B**, Confocal images showing expression of pWOX5:ER:GFP quiescent cells lineage marker in WT and blj jkd4 scr4 at 6dpi. White arrowhead: Quiescent cells. **C**, Confocal images showing expression of pWOX5:ER:GFP quiescent cells lineage marker in WT at 7dpi, at 5 dpi after treatment with bleomycin and after 48 hours of recovery. White arrowhead: Non-damage quiescent cells. **D**, Confocal image of blj jkd4 scr4 triple mutant at 12 dpi. Scale bars: 25 µm.

bioRxiv preprint doi: https://doi.org/10.1101/803973 This version posted October 14, 2019. The copyright holder for this preprint (which was not certified by peer review) is the author/funder. All rights reserved. No reuse allowed without permission.

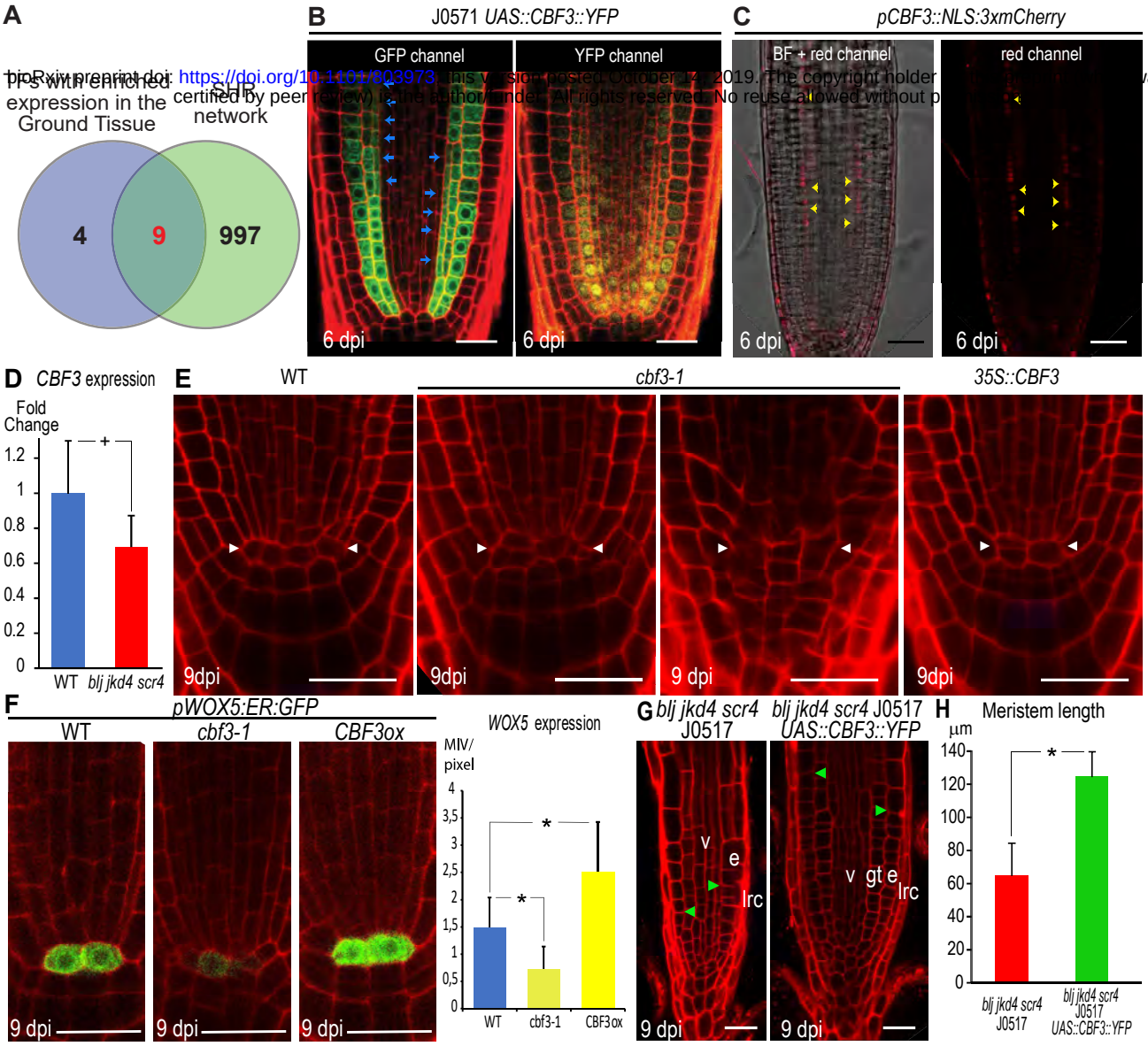

Fig. 4. C REPEAT BINDING FACTOR 3 (CBF3) moves out from the ground tissue and regulates stem cell niche differentiation and root radial pattern. **A**. venn diagram. **B**. confocal images showing localization of yellow fluorescet protein (YFP)-tagged CBF3 in the UAS/GAL4 system and enhancer trap line J0571, which drives expression to the ground tissue (GFP marked). Blue arrows: ectopics divisions in ground tissue. **C**. CBF3 promoter expression in the RAM. Yellow arrowheads: nuclear localized mCherry fluorescent protein under the control of CBF3 promoter. **D.** Real-time PCR analysis of CBF3 expression in WT and *blj jkd4 scr4* RAMs at 6 dpi. Cross: p-valu<0.05 in a one-way ANOVA. **E**. confocal images of the stem cell niche of WT, cbf3-1 and *p35S:CBF3* at 9dpi. **F**, Confocal images showing the expression of *pWOX5:ER:GFP* in WT, cbf3-1 and *p35S:CBF3* plants at 9dpi. Graph comparing the expression of *pWOX5:ER:GFP* in WT and blj jkd4 scrc4 plants at 9dpi. **G**. confocal images at 9 dpi of the RAM of blj jkd4 scr4 J0571 and UAS:CBF3:eYFP introgressed into blj jkd4 scr4 J0571. Lrc: lateral root cap, e: epidermis, gt: ground tissue, v:vasculature. Green arrowheads: end of the meristem. H, Meristem size of blj jkd4 scr4 J0571 and UAS:CBF3:eYFP at 9dpi. Asterisk: p-value<0,001 in a one-way ANOVA. MIV/pixel: mean intensity value/pixel. Scale bars: 25um

bioRxiv preprint doi: https://doi.org/10.1101/803973; this version posted October 14, 2019. The copyright holder for this preprint (which was not certified by peer review) is the author/funder. All rights reserved. No reuse allowed without permission.

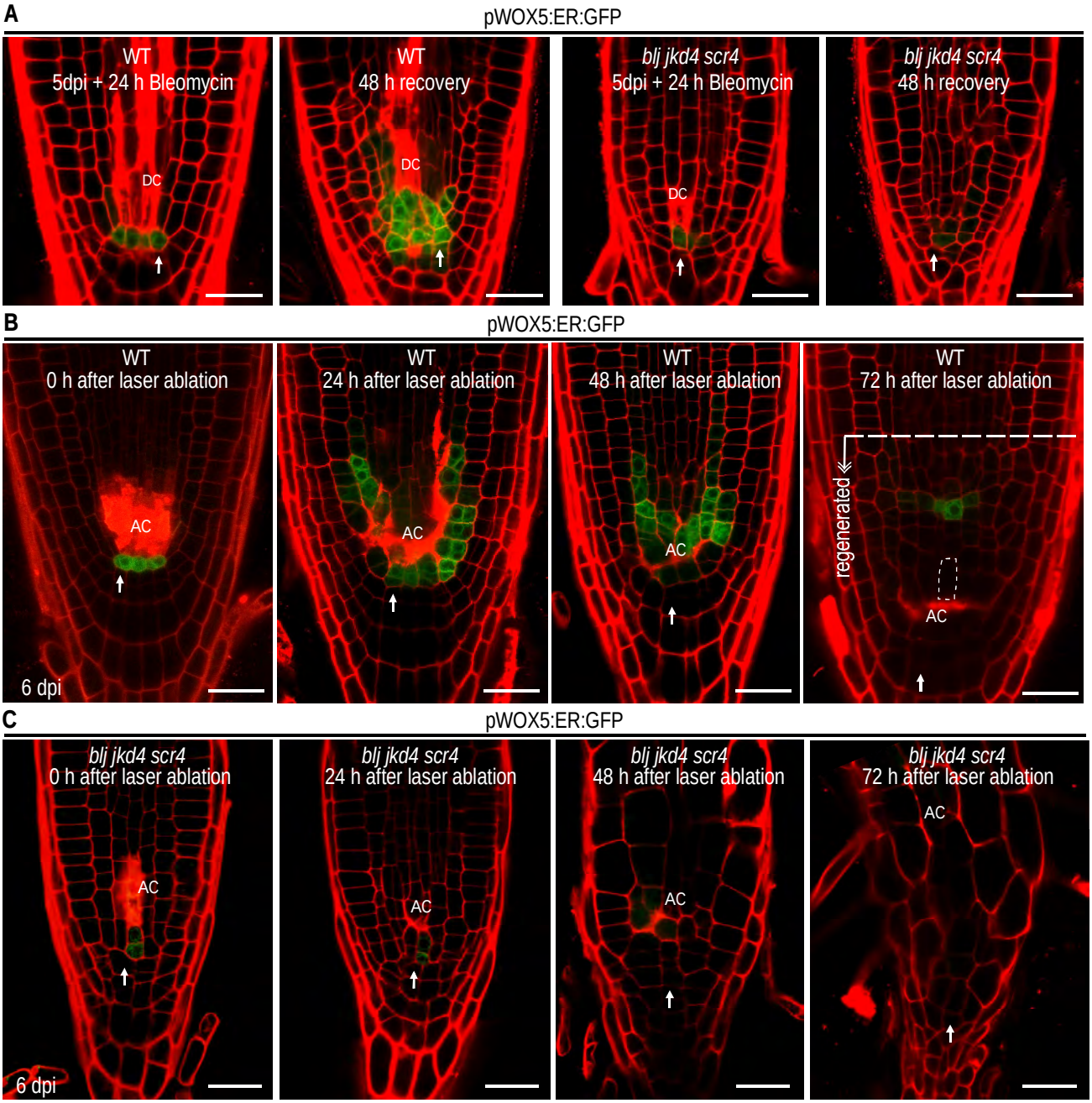

Fig. 5. *BLUEJAY, JACKDAW and SCARECROW* are required for quiescent center mediated regeneration and stem cell niche formation. A, confocal 48-hours (h)-time-lapse images of stem cell niche regeneration upon low dose of bleomycin treatment (0.8 ug/mL). WT and *blj jkd4 scr4* roots carrying the *pWOX5:ER:GFP* QC marker were treated for 24h and then moved to bleomycin-free medium to asses recovery. **B-C**, confocal 72h-time-lapse images of stem cell niche regeneration upon laser ablation of stem cells above the QC, in WT and *blj jkd4 scr4* roots carrying the *pWOX5:ER:GFP* QC marker. AC: ablated cells. Dashed line: elongated cells (twice the size than adjacent upper cells). White arrow: follow-up during regeneration of an adjacent cell lower to QC at the time of ablation. Scale bars: 25µm.

bioRxiv preprint doi: https://doi.org/10.1101/803973; this version posted October 14, 2019. The copyright holder for this preprint (which was not certified by peer review) is the author/funder. All rights reserved. No reuse allowed without permission.

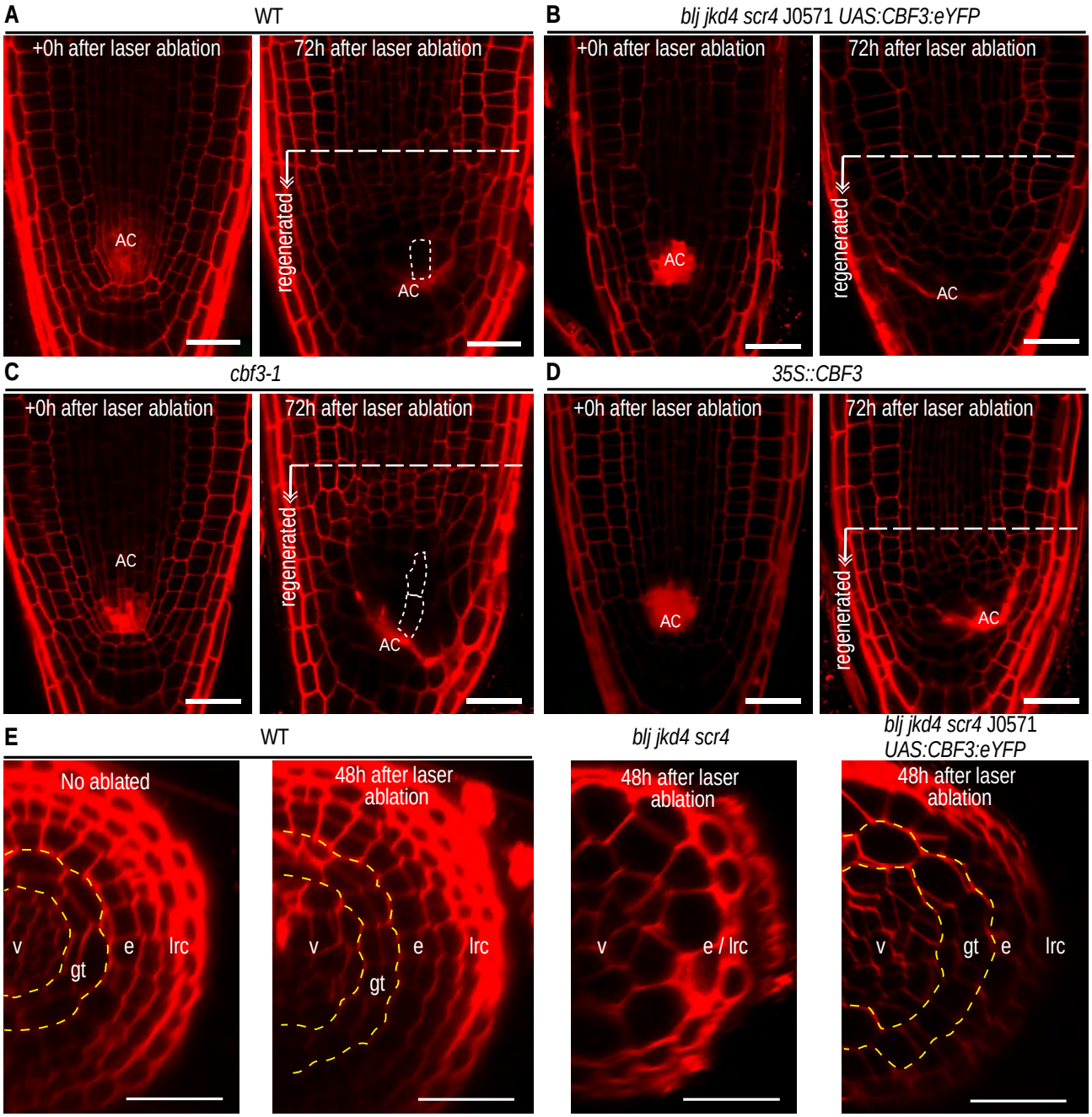

Fig. 7. CBF3 regulates stem cell niche specification and root patterning during regeneration. **A-D**, confocal images of stem cell niche regeneration upon laser ablation of cells above the QC, in WT, *blj jkd4 scr4*, *blj jkd4 scr4* J0571 *pUAS:CBF3:eYFP*, *cbf3-1* and *35S::CBF3* seedlings at 0 and 72h after laser ablation. AC: ablated cells. Dashed line: elongated cells (twice the size than adjacent upper cells). **E**, confocal images of root cross-sections above the QC at 48h after ablation. lrc: lateral root cap, e: epidermis, gt: ground tissue, v:vasculature. Dashed yellow line: contour delimiting the ground tissue. Scale bars: 25µm.